

New Zero-Velocity Detector for Low-Cost Inertial Pedestrian Navigation

Muhammad Syahmi Hamdan¹, Khairi Abdulrahim^{1,*}

¹ Department of Electrical and Electronic Engineering, Faculty of Engineering and Built Environment, Universiti Sains Islam Malaysia, 71800 Nilai, Negeri Sembilan, Malaysia

ABSTRACT

A new Zero Velocity Interval (ZVI) detector is proposed and investigated in this article to augment the computation of a pedestrian's position. In a low-cost pedestrian navigation system, the position of a pedestrian can be computed by using inertial navigation algorithms. The low-cost pedestrian navigation system employs an inertial measurement unit (IMU) comprised of accelerometer and gyroscope sensors to record acceleration and attitude rate. These measurements, when integrated mathematically, yield velocity and position. Similarly, attitude rate changes to attitude. The algorithm will then be able to figure out the changes in pedestrian position with the proper attitude. However, due to its low-cost nature, these sensors are built in such a way that their measurements are easily corrupted by noise, and once integrated mathematically, the measurement error grows exponentially. Zero Velocity Update (ZUPT) algorithm is frequently used to limit these errors. It works by detecting the ZVI that occur when the foot is on the ground. Assuming that the foot on the ground should have zero velocity, any remaining velocity measurements detected during this period are considered an error and are fed back to the navigation algorithm for correction. To detect the ZVI, a few commonly used detectors, namely Angular Rate Energy (ARE), Acceleration Moving Variance (MV), Acceleration Magnitude (MAG), and Generalized Likelihood Ratio Test (GLRT) were revisited. These detectors were tested with real-world datasets of walking pedestrians. Then, a new detector, the Angular Rate Moving Variance (ARMV) detector, is proposed, and its performance is compared to that of the existing detectors.

Keywords:

Low-cost; real-time; portable; water
quality monitoring system; water
pollution

Received: 3 October 2021

Revised: 15 January 2022

Accepted: 20 January 2022

Published: 25 January 2022

1. Introduction

The pedestrian navigation field is gaining interest in research because it can be improved to better detect and determine the location of someone, particularly in an indoor environment and in rural areas. For someone who is unfamiliar with the area, a pedestrian navigation system (PNS) can be very useful in updating his current location in real-time [1]. This can be accomplished by utilising various navigation technologies commonly used in this system, such as the Global Navigation Satellite System (GNSS), the self-contained sensor, and the radio frequency (RF) signal. However, these technologies have some flaws that make them unsuitable for use in an indoor environment.

* Corresponding author.

E-mail address: khairiabdulrahim@usim.edu.my

<https://doi.org/10.37934/araset.26.2.823>

Because the signal is blocked by the wall, the GNSS signal cannot be used to detect position in an indoor environment, and the RF signal output has some error due to the nature of the integration [2]. These technologies' flaws can be overcome by combining them with other positioning technology, referred to as microelectromechanical systems (MEMS). The combination of these two technologies improves the efficiency with which pedestrians in an indoor environment can be located. The Inertial Measurement Unit (IMU) is a microelectromechanical system (MEMS) that consists of gyroscope and accelerometer sensors. It functions as a sensor to detect changes in velocity measurement that occur during a pedestrian's walking cycle, and the velocity can be integrated mathematically to yield position. It is widely used and developed in navigation systems because it is a low-cost device that is simple to implement for the pedestrian user [3]. The velocity measurement output from this sensor still has some errors, but there is a technique called a Zero-velocity UPdaTe (ZUPT) that can help reduce the errors. The ZUPT technique uses an algorithm to detect the zero-velocity condition that occurs during the walking cycle [4].

The stance and swing phases of a pedestrian alternate during the walking cycle, and these phases can be classified into four different states. A swing phase occurs when the foot is not touching the ground and the velocity is greater than zero, whereas a stance phase occurs when the foot is touching the ground but not moving. Figure 1 depicts the condition of the foot in the stance phase, whereas states 2 and 3 depict the condition of the foot as it begins to move and swing again. State 4 depicts the condition of the foot as it begins to touch the ground once more before returning to state 1. The mechanism of these 4 alternately occurring states produces a short period in state 1 where the velocity is approximately zero, which is known as the Zero Velocity Interval (ZVI) [3].

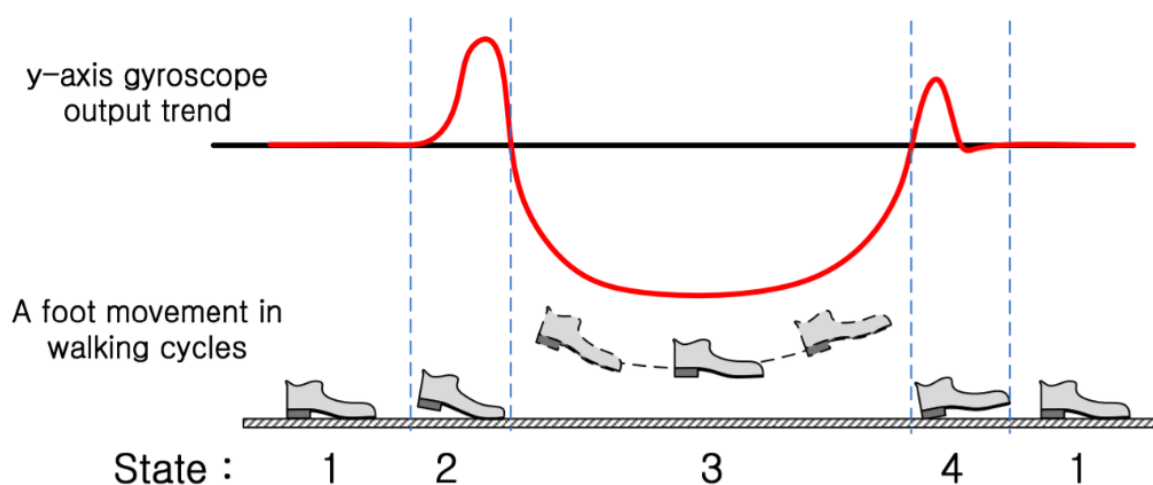


Fig. 1. Value trend of y-axis gyroscope and foot movement in gait cycle [4]

The performance of the detectors in detecting zero-velocity intervals is used to evaluate the ZUPT. Several detectors, such as the angular rate energy (ARE) detector, acceleration moving variance (MV) detector, acceleration magnitude (MAG) detector, and the stance hypothesis optimal (SHOE) detector, have been used in previous projects to detect the zero-velocity interval (ZVI). Each detector is made up of various algorithms and threshold values that are empirically determined based on the pedestrian's velocity. Using the algorithms of these detectors, the velocity measurements recorded by the gyroscope and accelerometer sensors were combined.

Each detector's algorithm is used to compute the values of the recorded data gait speed, and the calculated values are then plotted. Following the plotting, the threshold value is applied to determine

whether the values fall below the threshold or not. If the statistical values are less than the threshold, the inertial measurement unit (IMU) is considered to be in zero-velocity mode; if the values are greater than the threshold, the IMU is not considered to be in zero-velocity mode. The zero-velocity update (ZUPT) is plotted when the observation is completed based on the detection of zero-velocity conditions. ZUPT plots 0 for zero velocity or stance phase and 1 for swing phase. A zero-velocity interval is defined as the point on the ZUPT graph where the values fall to 0 before rising to 1. The successfully detected zero-velocity intervals are then used to plot the trajectory point.

In this article, a new zero velocity detector and threshold value are proposed to better detect zero velocity intervals at low gait speed, and the detector's efficiency is compared to that of the angular rate energy (ARE), acceleration moving variance (MV), acceleration magnitude (MAG), and stance hypothesis optimal (SHOE) detectors.

2. Methodology

Previously, the Global Positioning System (GPS) was used in conjunction with other navigation systems to detect the location of the pedestrian [5,6] and [7]. The integration of GPS with other navigation systems improves pedestrian navigation accuracy. There were also some works in Serra *et al.*, [8], Zhuang *et al.*, [9], Examiner *et al.*, [10], and Schougaard *et al.*, [11] in which the smartphone was outfitted with an additional navigation system. The dead reckoning positioning step, microelectromechanical sensors (MEMS), and GPS were all part of the navigation system. It aided in the establishment of a communication link between the communication server and the device itself for the location to be updated on a regular basis. In Abdulrahim *et al.*, [3,12], the inertial measurement unit (IMU) was used to collect data on the pedestrian's gait speed, acting as a sensor comprised of an accelerometer and gyroscope capable of sensing changes in velocity while walking. The INS module, gait phase detection module, and zero velocity update module were proposed as online smoothing zero-velocity update (ZUPT) modules [13]. Previous detectors such as ARE, MV, and MAG detectors were tested to investigate the framework for each detector, and a new algorithm with the integration of zero velocity update (ZUPT) was proposed [14].

The goal of this work is to propose a new velocity detector algorithm that can be used for pedestrian navigation using zero-velocity update (ZUPT). The MATLAB application was used to run the coding and display the output in detecting the zero-velocity interval (ZVI) at low gait speed data in this project. The data for this work was obtained from the OpenShoe project, which was started by researchers from the department of signal processing at KTH Royal Institute of Technology [15]. A set of algorithm frameworks was provided for this work, and it was used to process the data. The Generalized Likelihood Ratio Test (GLRT), Acceleration-Moving Variance (MV), Acceleration-Magnitude (MAG), Angular Rate Energy (ARE), and the proposed Angular Rate Moving Variance (ARMV) detectors are used in this project to compute gait speeds and determine the zero-velocity condition for the zero-velocity update.

2.1 Understanding the process flow of Generalized Likelihood Ratio Test (GLRT), Acceleration-Moving Variance (MV), Acceleration-Magnitude (MAG), Angular Rate Energy (ARE) detectors

The detectors were tested using the Generalized Likelihood Ratio Test (GLRT), Acceleration-Moving Variance (MV), Acceleration-Magnitude (MAG), and Angular Rate Energy (ARE) to understand the process flow of the detectors in detecting the stance phase and to evaluate the overall performance of the detectors. For each detector, the algorithms in sections 2.1.1, 2.1.2, 2.1.3, and 2.1.4 were used to compute the gait speeds recorded and plot the test statistics.

The test statistic, T, values were then compared with the threshold value set for these detectors to determine the condition of the foot at that time. If the values obtained fell below the threshold, the hypothesis states that the IMU is in a stationary phase, and if the values calculated do not fall below the threshold, the hypothesis concludes that the IMU is in the swing phase. The graph of zero-velocity update (ZUPT) can be plotted between 0 and 1 based on the observation. In the graph, values that are less than the threshold are plotted as 0, while values that are greater than the threshold are plotted as 1, and the plotting of these values alternates, forming periods. Zero-velocity intervals are the brief periods when the value falls to 0 before rising back to 1. The detection of the zero-velocity interval is then used for trajectory plotting. The detector that correctly detects zero-velocity intervals generates a good trajectory pattern that depicts a pedestrian's path.

2.1.1 Generalized Likelihood Rate Tests (GLRT) Detector

$$T(z_n) = \frac{1}{N} \sum_{k \in \Omega_n} \left(\frac{1}{\sigma_a^2} \|y_k^q\|^2 - g \frac{y_\eta^q}{\|\bar{y}_{11}^a\|} + \frac{1}{\sigma_\omega^2} \|y_k^\omega\|^2 \right) < \gamma \quad (1)$$

The algorithm for the GLRT detector shows the summation of the mean square error of fitting a vector of magnitude g with the direction of the average specific force vector to the accelerometer data and the energy in the gyroscope signal. If the measurement that is obtained falls below the threshold, the algorithm concludes the hypothesis that IMU is stationary [14].

2.1.2 Acceleration Magnitude (MAG) Detector

$$Tm(z_n^a) = \frac{1}{\sigma_a^2 N} \sum_{k \in \Omega_n} (\|y_k^q\| - g)^2 < \gamma \quad (2)$$

The algorithm for this detector is described as the summation of the difference between the magnitude of the accelerometer signal with gravity. If the values of measurement fall below the threshold, the values are considered as zero-velocity [14].

2.1.3 Angular Rate Energy (ARE) Detector

$$T\omega(z_n^\omega) \frac{1}{N} \sum_{k \in \Omega_n} (\|y_k^\omega\|^2 < \gamma_\omega \quad (3)$$

The algorithm for this detector is described as the summation of the magnitude of the gyroscope signal. If the values of measurement fall below the threshold, the values are considered as zero-velocity [14].

2.1.4 Acceleration-Moving Variance (MV) Detector

$$Tv(z_n^a) = \frac{1}{N} \sum_{k \in \Omega_n} (\|y_k^q - y_\eta^q\|^2 < \gamma \quad (4)$$

The algorithm for this detector is described as the summation of the magnitude between the difference of angular signal and the value of the mean of angular data. If the values calculated from this measurement fall below the threshold, the value is considered in a stance phase [14].

2.2 Angular Rate Moving Variance (ARMV) detector

An angular rate moving variance (ARMV) detector is proposed as a new zero-velocity detection algorithm. The detector's algorithm is shown in section 2.2.1, where the gyroscope values are chosen to be computed using the proposed algorithm and detecting the zero-velocity condition. The values are loaded into the ARMV detector's function, and the test statistic, T , is calculated and plotted.

2.2.1 Angular Rate Moving Variance (ARMV) Detector

$$Tv(z_n^a) = \frac{1}{N} \sum_{k \in \Omega_n} \|y_k^\omega - y_n^\omega\|^2 < \gamma \quad (5)$$

The algorithm for this detector is described as the sum of the magnitudes of the gyroscope signal difference and the value of the gyroscope signal mean. If the statistical values calculated from this measurement are less than the threshold, the value is regarded as zero-velocity. During the early stages, no fixed threshold value is set for this detector because the algorithm of this detector must be tested with multiple threshold values until the best result is obtained.

2.2.2 Set the best threshold value for the Angular Rate Moving Variance (ARMV) detector

The threshold for this detector is being tested with values of 10000, 1000, 100, 10, 1, 0.5, and 0.1. The horizontal and spherical errors calculated from the plotted trajectories, as well as the pattern of the trajectories themselves, are used to evaluate these values. The threshold for the ARMV detector is set to the value that produced the lowest spherical and horizontal errors as well as the best trajectory pattern. Based on the results of the evaluation, 0.5 produced the best output, indicating that this value can be used to detect the zero-velocity condition.

2.2.3 Plotting of test statistic, T of Angular Rate Moving Variance (ARMV) detector

The proposed algorithm for the angular rate moving variance (ARMV) detector is used to compute the gyroscope values that represent the recorded velocity speed. The calculated statistical values are plotted to form a speed graph. The threshold value set for this detector is applied to the graph to determine whether the calculated values fall below or exceed the threshold. The graph of the zero-velocity update can be plotted based on this evaluation.

2.2.4 Plotting of zero-velocity update (ZUPT) of Angular Rate Moving Variance (ARMV) detector

The applied zero-velocity update (ZUPT) is plotted based on statistical values that are checked against the threshold value. In zero-velocity update (ZUPT), values that are less than the threshold are considered 0 and values that are greater than the threshold are considered 1. The plotting of the zero-velocity update (ZUPT) used reveals that the values fluctuate between 0 and 1. The zero-velocity

intervals (ZVI) are defined as the period during which the velocity falls to 0 before rising to 1, and these intervals alternate.

2.2.5 Plotting of zero-velocity update (ZUPT) of Angular Rate Moving Variance (ARMV) detector

The trajectory of the angular rate moving variance (ARMV) is then plotted from the detector's zero-velocity update (ZUPT). The coordinates of the trajectory's starting and ending points are observed in order to compare the distance between these two detector points. A shorter distance between these two points demonstrated that the proposed detector is detectable in zero-velocity intervals.

2.2.6 The calculation of Euclidean Distance Error

Calculating Euclidean distance error's function is to find the error in the distance between two coordinates. The Euclidean distance error is calculated using the coordinates of the final and initial points for the angular rate moving variance (ARMV) detector, angular rate energy (ARE), acceleration moving variance (MV), acceleration magnitude (MAG), and generalised Likelihood Ratio Test (GLRT). The performance of these detectors in detecting zero velocity intervals can be evaluated by calculating this error using the equation below. When compared to the detector that produces a higher distance error, the detector that produces a lower distance error performs better.

$$\text{Euclidean Distance Error} = \sqrt{(x_2 - x_1)^2 + (y_2 - y_1)^2} \quad (6)$$

3. Results

The results are divided into five sections: calculated horizontal and spherical positioning errors, test statistic plotting, zero-velocity update (ZUPT) plotting, trajectory point plotting, and detector position accuracy.

3.1 Horizontal and Spherical Positioning Error

The horizontal and spherical errors are calculated using different threshold values to set a new threshold value for the proposed angular rate moving variance (ARMV) detector. The threshold value for the ARMV detector is determined by calculating the errors and selecting the threshold value that produces the lowest error. Table 1 displays various values of the error calculated using different threshold values. There are 5 threshold values in the table that produce a considerably low error (< 2 m), and the values are further evaluated by observing the plotted trajectories. The ARMV detector is run using these threshold values for the second evaluation, and the trajectories plotted for each threshold value are observed. Based on the trajectories plotted in table 2, threshold value 0.5 produced the best trajectory because this value can be used to detect zero velocity intervals with this detector.

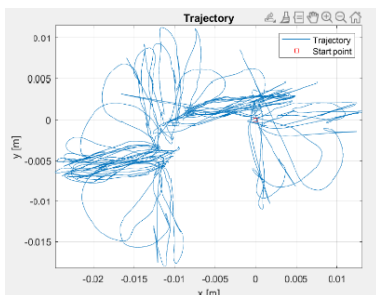
Table 1

Horizontal and spherical errors calculated by using different threshold values for ARMV detector

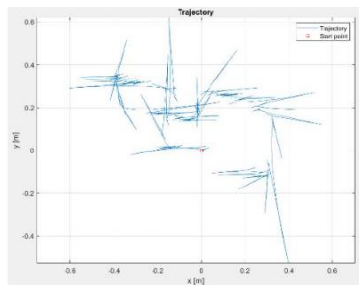
Detector	Threshold, γ	Horizontal Error (m)	Spherical Error (m)
ARMV	10000	0.010186	0.010912
ARMV	1000	0.25275	0.29244
ARMV	100	0.74536	1.2563
ARMV	10	6.8897	7.3069
ARMV	1	0.82935	1.993
ARMV	0.1	1.8041	2.1086
ARMV	0.5	0.09315	1.2284

Table 2

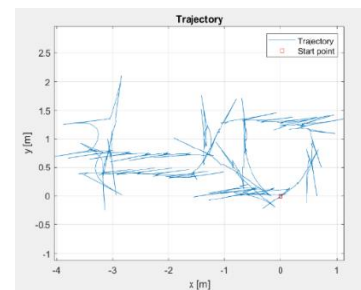
Trajectories plotted using selected threshold values



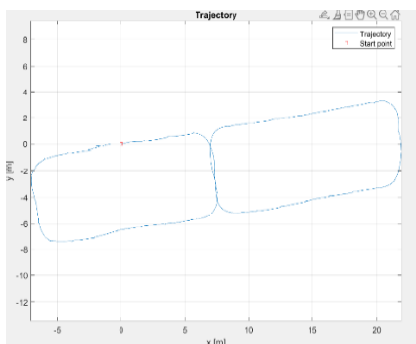
$\lambda = 10000$



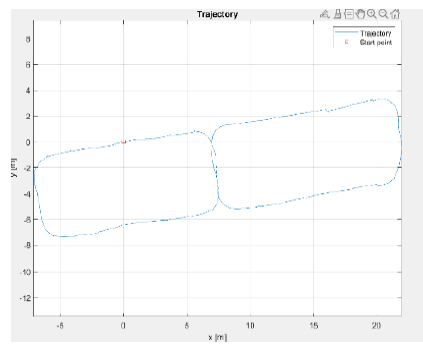
$\lambda = 1000$



$\lambda = 100$



$\lambda = 1$



$\lambda = 0.5$

3.2 The Comparison of the Plotting of the Test Statistics, T for the Detectors

The pattern of the graphs is used to evaluate the plotting of the test statistic, T , for the Generalized Likelihood Ratio Test (GLRT), Acceleration-Moving Variance (MV), Acceleration-Magnitude (MAG), Angular Rate Energy (ARE), and Angular Rate Moving Variance detectors. The graph's pattern is determined by the values calculated by the various algorithms for each detector. Figures 2, 3, 4, 5 and 6 in this section depict the pattern of the graph of the test statistic, T , plotted for GLRT, MV, MAG, ARE, and ARMV detectors. In previous research, the GLRT detector was declared the best detector for detecting zero-velocity intervals, and therefore the performance of the ARMV detector was compared with that of the GLRT detector. The graph pattern for the GLRT detector in figure 2 decreased to zero and then increased. According to the evaluation, the ARMV detector has a similar pattern to the GLRT detector in that the velocity values appear to approach zero for a short time before rising again. The ARMV detector produced a similar pattern, demonstrating that the proposed algorithm and threshold can successfully calculate the gyroscope values recorded during the normal walking cycle and detect the zero-velocity condition.

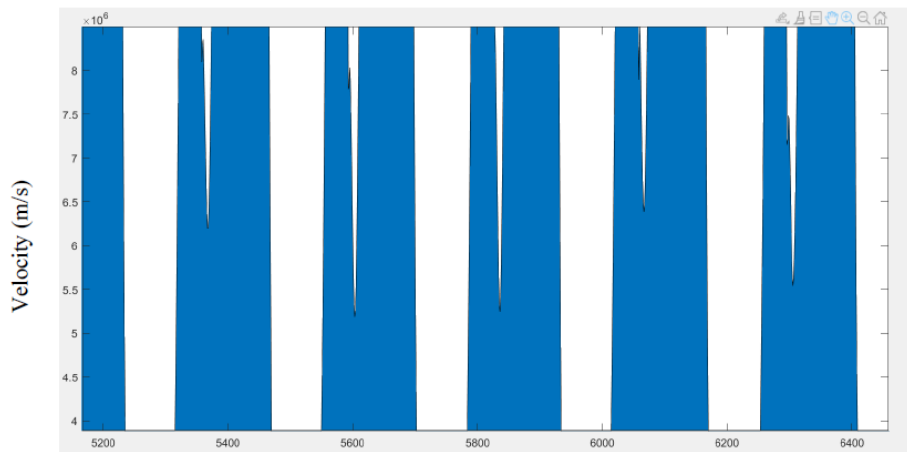


Fig. 2. T plot of GLRT detector

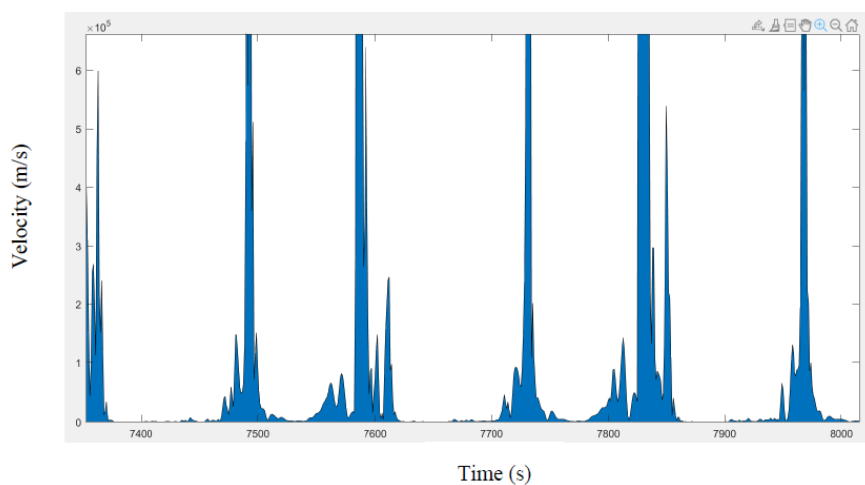


Fig. 3. T plot of MV detector

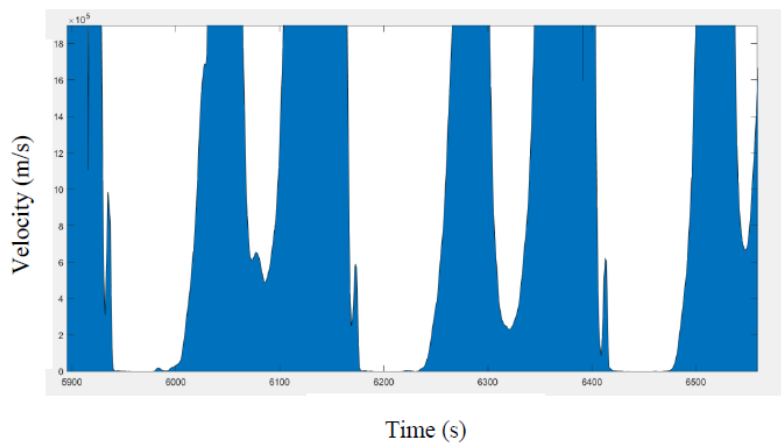


Fig. 4. T plot of MAG detector

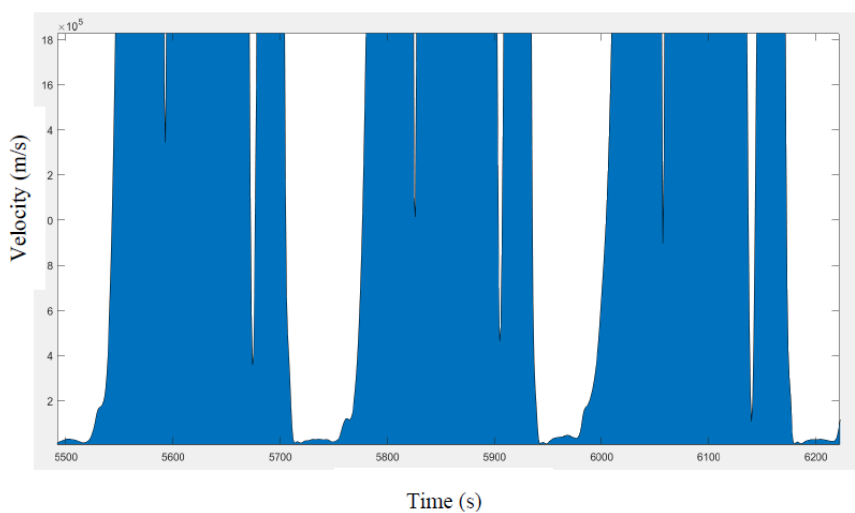


Fig. 5. T plot of ARE detector

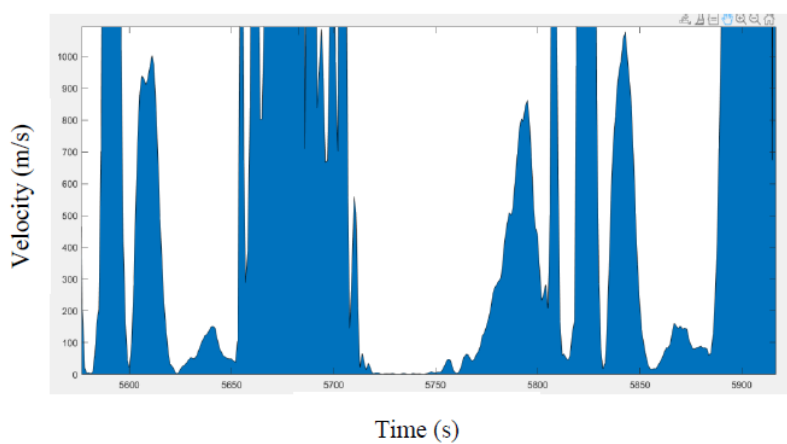


Fig. 6. T plot of the proposed ARMV detector

3.3 Graph of zero-velocity update (ZUPT) plotted for angular rate energy (ARE), acceleration moving variance (MV), acceleration magnitude (MAG), generalized like hood Ratio Test (GLRT), and angular rate moving variance (ARMV) detectors

After the statistical values are combined with the threshold value, the graph of zero-velocity update (ZUPT) for the five detectors is plotted. It demonstrates the detectors' accuracy in detecting the zero-velocity condition by observing the periods of velocity that fall to 0. Figures 7, 8, 9, 10, and 11 show the zero-velocity update (ZUPT) graph plotted for the five detectors. The graphs of ZUPT for GLRT, MAG, ARE, and ARMV detectors show a similar pattern, with the values of speed alternately changing between 0 and 1. The term "zero-velocity intervals" refers to short periods when the velocity remains zero before increasing to one. A detector with the incorrect algorithm and threshold settings resulted in false detection, as shown in figure 8, where the ZUPT graph is overlaid and the zero-velocity intervals cannot be detected.

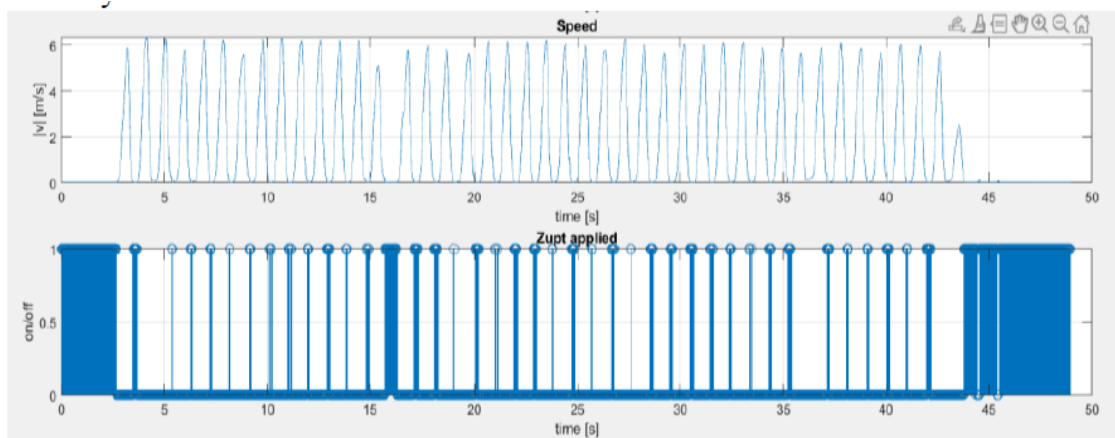


Fig. 7. ZUPT applied for GLRT detector

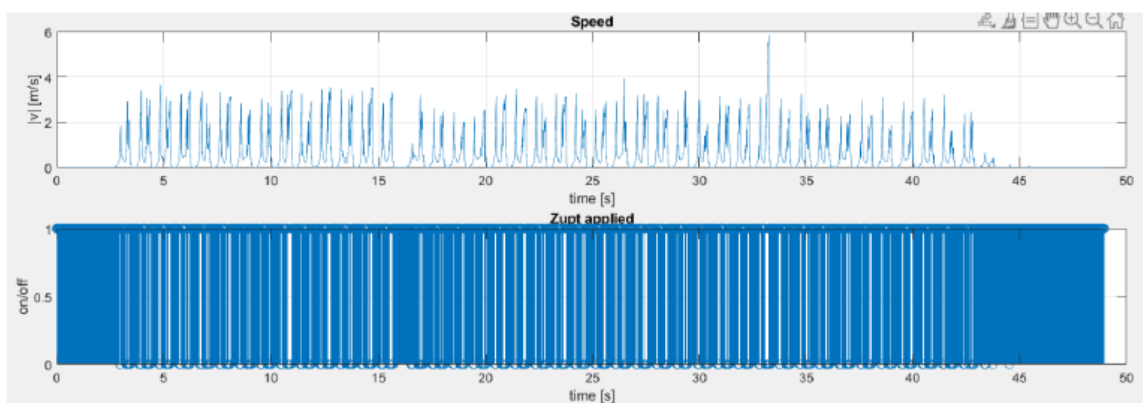


Fig. 8. ZUPT applied for MV detector

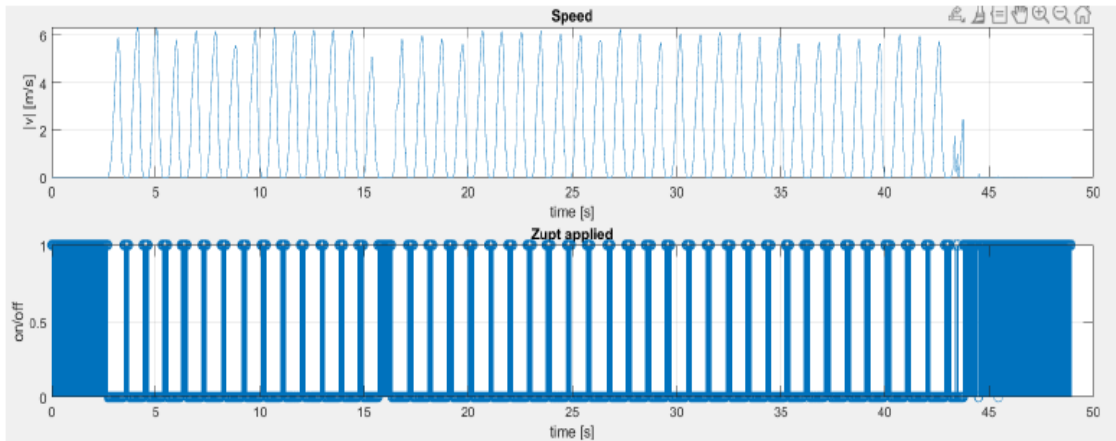


Fig.9. ZUPT applied for MAG detector

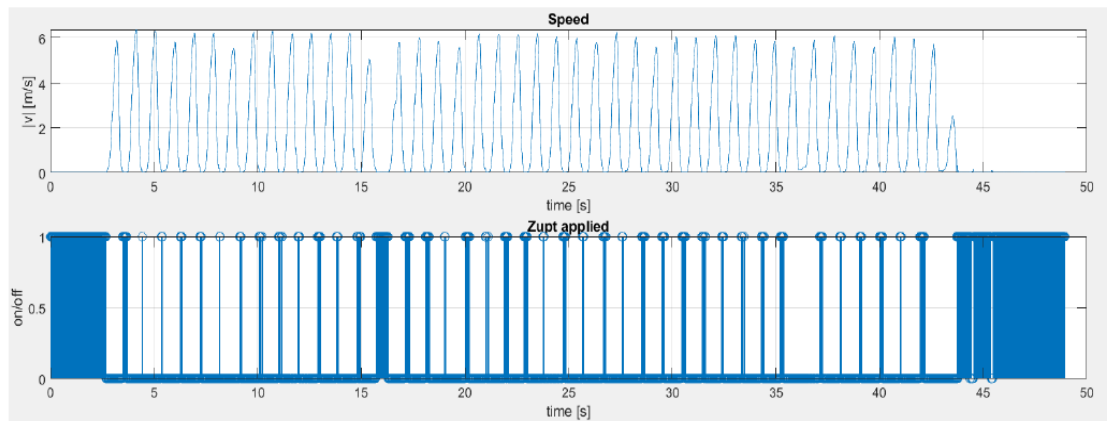


Fig.10. ZUPT applied for ARE detector

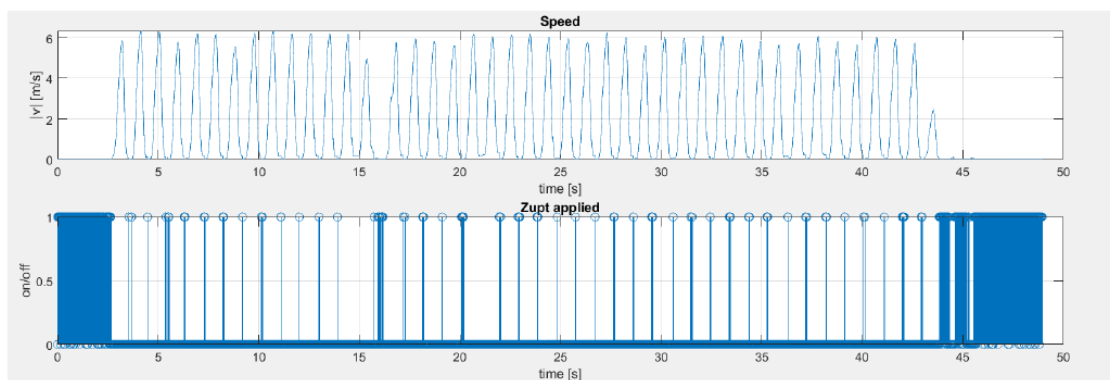
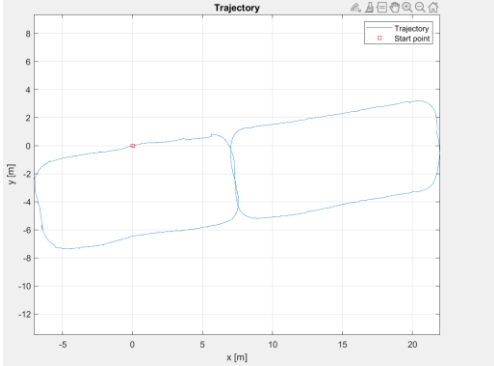
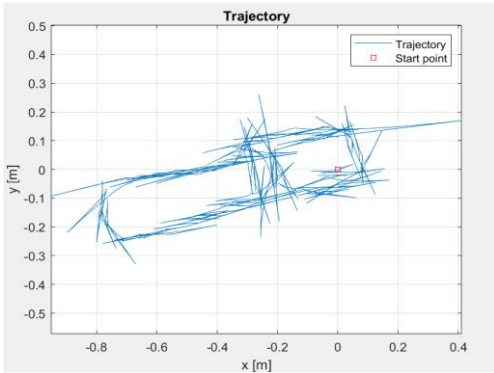


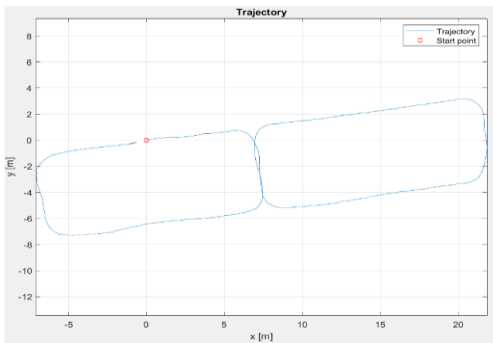
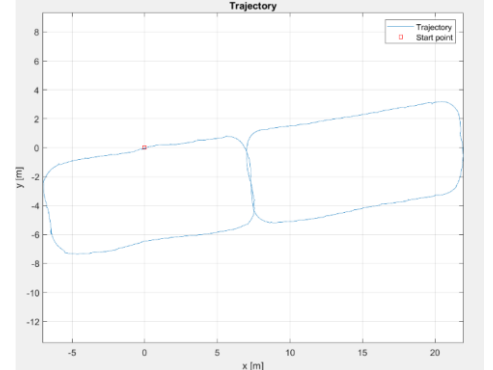
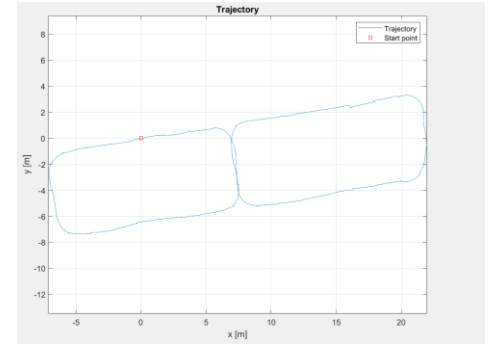
Fig.11. ZUPT applied for the proposed ARMV detector

3.4 The plotting of trajectory points for angular rate energy (ARE), acceleration moving variance (MV), acceleration magnitude (MAG), generalized like hood Ratio Test (GLRT), and angular rate moving variance (ARMV) detectors.

The trajectories plotted for the five detectors are evaluated by observing the pattern of the trajectories as well as the two points plotted in the trajectories that represent the final and starting points. Table 3 displays the trajectories plotted from the five detectors. According to the observations, the GLRT detector produced a better trajectory than the others. The points are well-placed and form a pattern that depicts the path of a walking pedestrian. The starting and ending points of the GLRT detector appeared to be the same (0,0). The performance of the ARE and ARMV detectors is similar because the pattern of the trajectories plotted is similar to that of the GLRT detector. However, the MV detector's trajectory point is not as smooth as the other detectors', and the endpoint for this trajectory cannot be defined. This is due to the MV detector's inability to detect zero-velocity intervals very well.

Table 3
 Trajectories plotted for the 5 detectors

Detectors	Trajectory plotted
<p>Generalized like hood Ratio Test (GLRT) detector.</p>	
<p>Acceleration moving variance (MV) detector.</p>	

<p>Acceleration magnitude (MAG) detector.</p>	
<p>Angular rate energy (ARE) detector.</p>	
<p>The proposed Angular rate moving variance (ARMV) detector.</p>	

3.5 Position accuracy of the angular rate energy (ARE), acceleration moving variance (MV), acceleration magnitude (MAG), generalized like hood Ratio Test (GLRT), and angular rate moving variance (ARMV) detectors

The positioning accuracy of the five detectors is calculated in order to compare their performance. The Euclidean distance error is calculated using the starting and ending points of the trajectory for each detector. Because each detector produced a unique value for the ending point, calculating the mean coordinate (x and y-axis) assisted in determining the final value of the ending point for each detector. Tables 4 and 5 show the mean coordinates of the final point for each detector, while table 6 shows the Euclidean distance error calculated from the values in tables 4 and 5. The GLRT detector determined the shortest distance between the final and initial points. Although

the ARMV detector produced better results compared to the MV and MAG detector, but GLRT and ARE detectors produced the best results.

Table 4
 Values of X-coordinate of the ending point for every detector

Detector	D1, m	D2, m	D3, m	D4, m	D5, m	D6, m	D7, m	D8, m	D9, m	D10, m	Mean of x-coordinate (m)
GLRT	-0.01	-0.15	-0.1	-0.12	-0.09	-0.1	-0.01	-0.03	0	-0.1	-0.071
MV	∞	∞	∞	∞	∞	∞	∞	∞	∞	∞	∞
MAG	-0.803	∞	∞	∞	∞	∞	∞	∞	∞	∞	-0.803
ARE	-0.159	-0.12	-0.1	-0.2	-0.1	-0.05	-0.04	-0.03	-0.02	-0.1	-0.0919
ARMV	-0.025	1.83	-1.5	-1.87	-0.2	-0.08	0.53	-2.1	0.56	0.01	-0.2845

Table 5
 Values of Y-coordinate of the ending point for every detector

Detector	D1, m	D2, m	D3, m	D4, m	D5, m	D6, m	D7, m	D8, m	D9, m	D10, m	Mean of y-coordinate (m)
GLRT	-0.04	0.37	0.4	0.26	0.18	0.39	0.4	0.43	0.2	0.37	0.296
MV	∞	∞	∞	∞	∞	∞	∞	∞	∞	∞	∞
MAG	-0.23	∞	∞	∞	∞	∞	∞	∞	∞	∞	-0.23
ARE	-0.114	0.32	0.4	0.3	0.18	0.38	0.45	0.43	0.2	0.37	0.2916
ARMV	-0.025	2.2	0.3	0.038	0.22	0.41	0.37	0.01	0.258	0.456	0.4237

Table 6
Euclidean distance error calculated

Detectors	Euclidian distance error (m)
GLRT	0.304
MV	∞
MAG	0.835
ARE	0.306
ARMV	0.510

To summarise this section, the proposed ARMV detector can be identified as a potential new detector in detecting the zero-velocity interval during normal walking gait. This is since it produces less error than the MV and MAG detectors used in this project. This is demonstrated by plotting the test statistic, the ZUPT, the trajectory point, and the error produced by the ARMV detector. This resulted in the conclusion that the threshold value set and the formulation used for this detector can adapt to different data speeds and are reliable for detecting the zero-velocity interval (ZVI).

4. Conclusions

In this article, a new zero velocity detector known as Angular Rate Moving Variance (ARMV) was proposed to detect the zero-velocity interval. The detector used the gyroscope measurements to calculate the pedestrian's data gait speed. A new threshold value was specified for the proposed detector to check the calculated gait speeds and identify the zero-velocity condition. The proposed detector was validated using the plotting of the test statistic, the zero-velocity update applied (ZUPT), the trajectories, and the computed Euclidean distance error. The Euclidean distance error was calculated from the trajectory plotting, and the accuracy of the proposed detector was determined. The acceleration-moving variance (MV) and acceleration magnitude (MAG) detectors were both outperformed by the proposed angular rate moving variance (ARMV) detector, although GLRT and ARE remains the best detector thus far in this work.

Acknowledgement

The research leading to this paper was financially supported by Universiti Sains Islam Malaysia through research code: PPPI/FKAB/0121/USIM/17321.

References

- [1] Huang, Hsiang-Yun, Chia-Yeh Hsieh, Kai-Chun Liu, Hui-Chun Cheng, Steen J. Hsu, and Chia-Tai Chan. "Multi-sensor fusion approach for improving map-based indoor pedestrian localization." *Sensors* 19, no. 17 (2019): 3786.
- [2] Tian, Xiaochun, Jiabin Chen, Yongqiang Han, Jianyu Shang, and Nan Li. "A novel zero velocity interval detection algorithm for self-contained pedestrian navigation system with inertial sensors." *Sensors* 16, no. 10 (2016): 1578.

- [3] Abdulrahim, Khairi, Terry Moore, Christopher Hide, and Chris Hill. "Understanding the performance of zero velocity updates in MEMS-based pedestrian navigation." *International Journal of Advancements in Technology* 5, no. 2 (2014).
- [4] Park, Sang Kyeong, and Young Soo Suh. "A zero velocity detection algorithm using inertial sensors for pedestrian navigation systems." *Sensors* 10, no. 10 (2010): 9163-9178.
- [5] Kourogi, Masakatsu, Nobuchika Sakata, Takashi Okuma, and Takeshi Kurata. "Indoor/outdoor pedestrian navigation with an embedded GPS/RFID/self-contained sensor system." In *International conference on artificial reality and telexistence*, pp. 1310-1321. Springer, Berlin, Heidelberg, 2006.
- [6] Yoon, Yong-Jin, King Ho Holden Li, Jiahe Steven Lee, and Woo-Tae Park. "Real-time precision pedestrian navigation solution using inertial navigation system and global positioning system." *Advances in Mechanical Engineering* 7, no. 3 (2015): 1687814014568501
- [7] Seitz, Jochen, Jasper Jahn, Javier Gutiérrez Boronat, Thorsten Vaupel, Steffen Meyer, and Jörn Thielecke. "A hidden markov model for urban navigation based on fingerprinting and pedestrian dead reckoning." In *2010 13th International Conference on Information Fusion*, pp. 1-8. IEEE, 2010.
- [8] Serra, Alberto, Davide Carboni, and Valentina Marotto. "Indoor pedestrian navigation system using a modern smartphone." In *Proceedings of the 12th international conference on Human computer interaction with mobile devices and services*, pp. 397-398. 2010.
- [9] Zhuang, Yuan, and Naser El-Sheimy. "Tightly-coupled integration of WiFi and MEMS sensors on handheld devices for indoor pedestrian navigation." *IEEE Sensors Journal* 16, no. 1 (2015): 224-234.
- [10] P. Examiner, T. Q. Nguyen, and P. C. Vanderhye, "(12) United States Patent," vol. 2, no. 12, 2009.
- [11] Schougaard, Kari Rye, Kaj Grønbaek, and Tejs Scharling. "Indoor pedestrian navigation based on hybrid route planning and location modeling." In *International Conference on Pervasive Computing*, pp. 289-306. Springer, Berlin, Heidelberg, 2012.
- [12] Abdulrahim, Khairi, Chris Hide, Terry Moore, and Chris Hill. "Aiding MEMS IMU with building heading for indoor pedestrian navigation." In *2010 ubiquitous positioning indoor navigation and location based service*, pp. 1-6. IEEE, 2010.
- [13] Zhao, Hongyu, Zhelong Wang, Qin Gao, Mohammad Mehedi Hassan, and Abdulhameed Alelaiwi. "Smooth estimation of human foot motion for zero-velocity-update-aided inertial pedestrian navigation system." *Sensor Review* (2015).
- [14] Skog, Isaac, John-Olof Nilsson, and Peter Händel. "Evaluation of zero-velocity detectors for foot-mounted inertial navigation systems." In *2010 International Conference on indoor positioning and indoor navigation*, pp. 1-6. IEEE, 2010.
- [15] Nilsson, John-Olof, Isaac Skog, Peter Händel, and K. V. S. Hari. "Foot-mounted INS for everybody-an open-source embedded implementation." In *Proceedings of IEEE/ION PLANS 2012*, pp. 140-145. 2012.